

Supporting Information

Improved Charge Carrier Dynamics in Polymer/Perovskite Nanocrystal Based Hybrid Ternary Solar Cells

Rezvan Soltani^{*,‡}, Bianka M.D. Puscher[‡], Ali Asghar Katbab^{*}, Ievgen Levchuk, Negar Kazerooni, Nicola Gasparini, Nadia Camaioni, Andres Osvet, Mirosław Batentschuk, Rainer H. Fink, Dirk M. Guldi, Tayebeh Ameri^{*}

[‡] Both authors contribute to the same parts to the paper

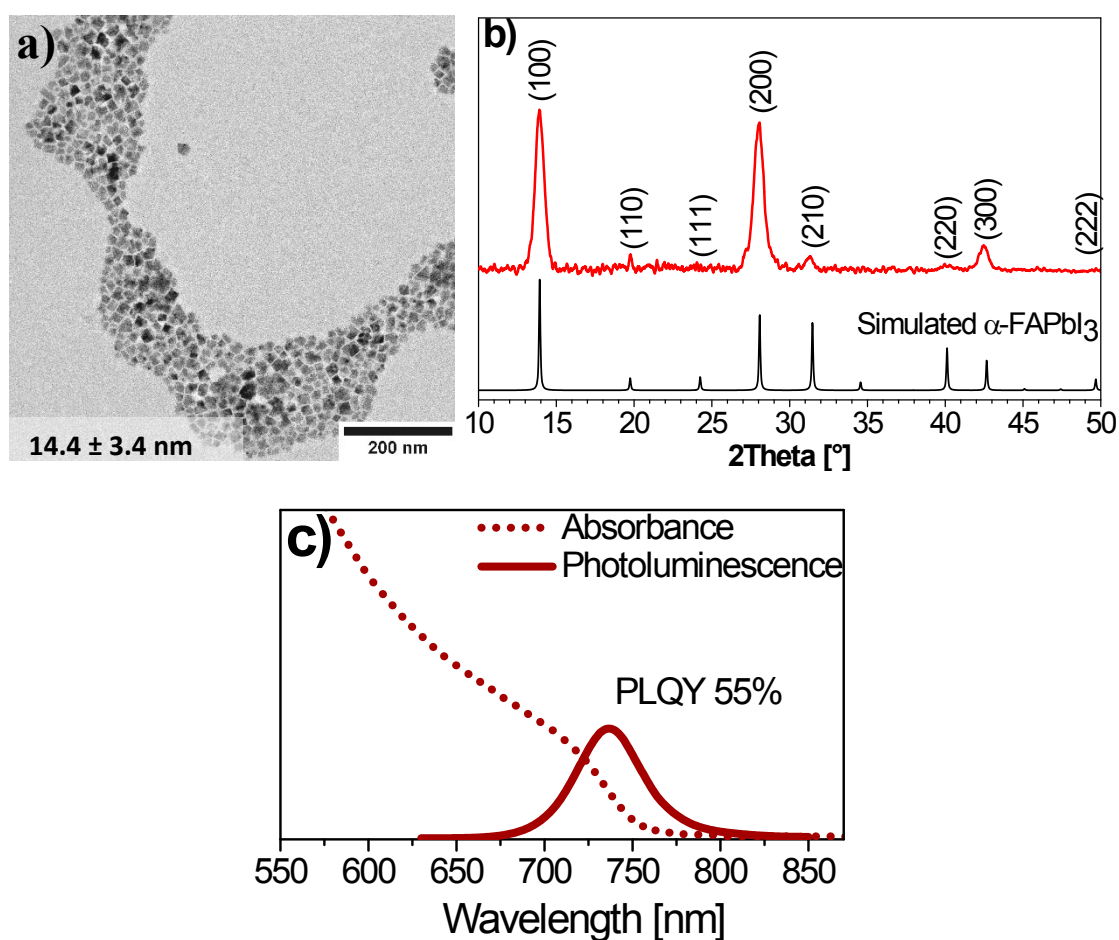


Figure S1. a) TEM micrograph of the monolayer Organolead Iodide Perovskite NCs on a grid. b) XRD of the α -FAPbI₃ Perovskite NCs sample. Simulated data are based a reference for cubic “black” α -phase from Stoumpos et al. (Inorg. Chem. 2013, 52, 9019-9038.) and c) Absorbance and photoluminescence spectra FAPbI₃ NCs in toluene solution.

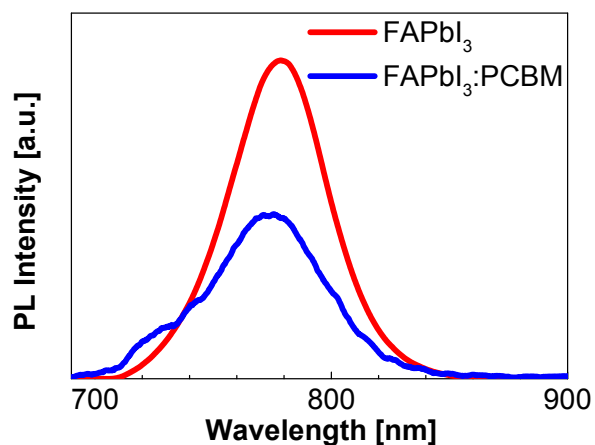


Figure S2. PL spectra of the films comprising FAPbI₃ and FAPbI₃:PCBM (1:1 weight ratio).

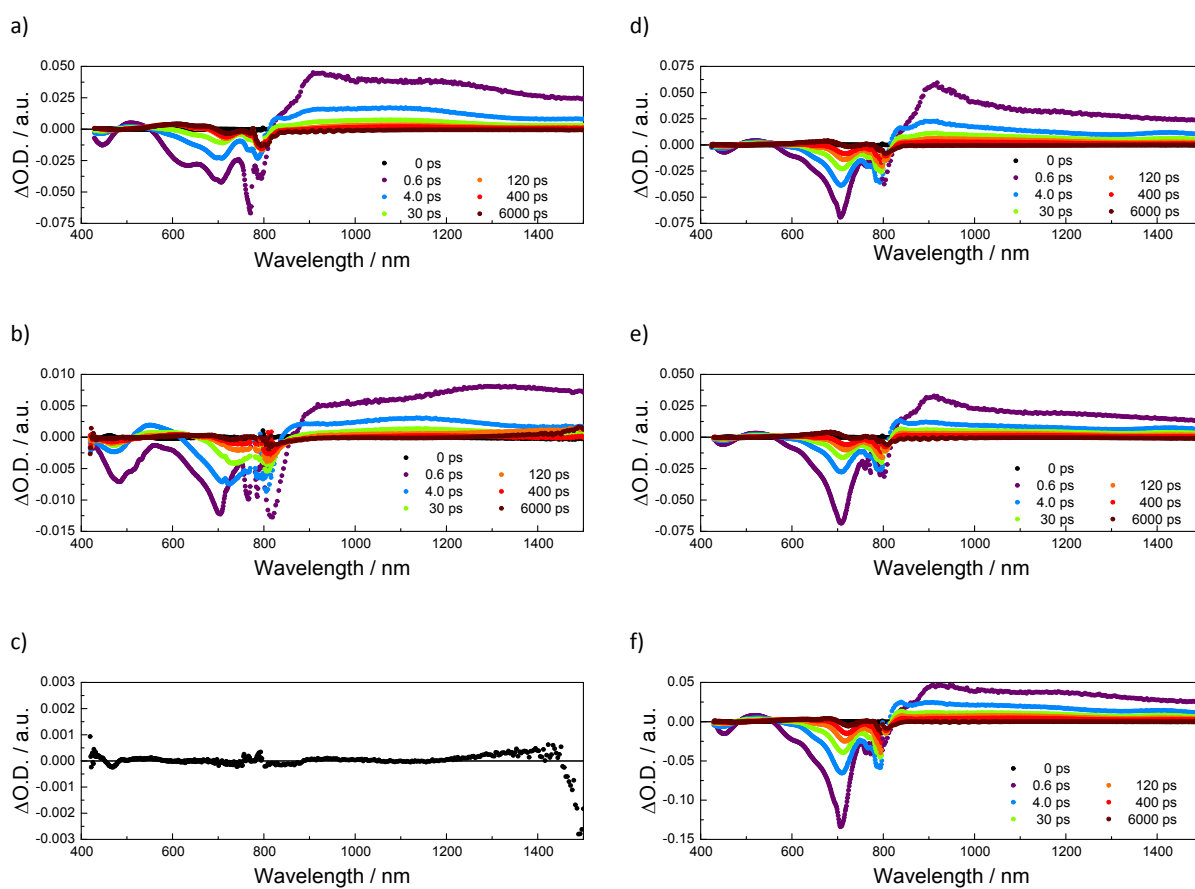


Figure S3. Differential absorption spectra obtained from femtosecond pump-probe experiments (775 nm) under inert atmosphere at room temperature of a) DPP; b) the binary blends DPP:FAPbI₃; c) PC61BM:FAPbI₃; d) and DPP:PC61BM; as well as of e) ternary blends comprising 5 and f) 10 wt.% FAPbI₃ NCs.

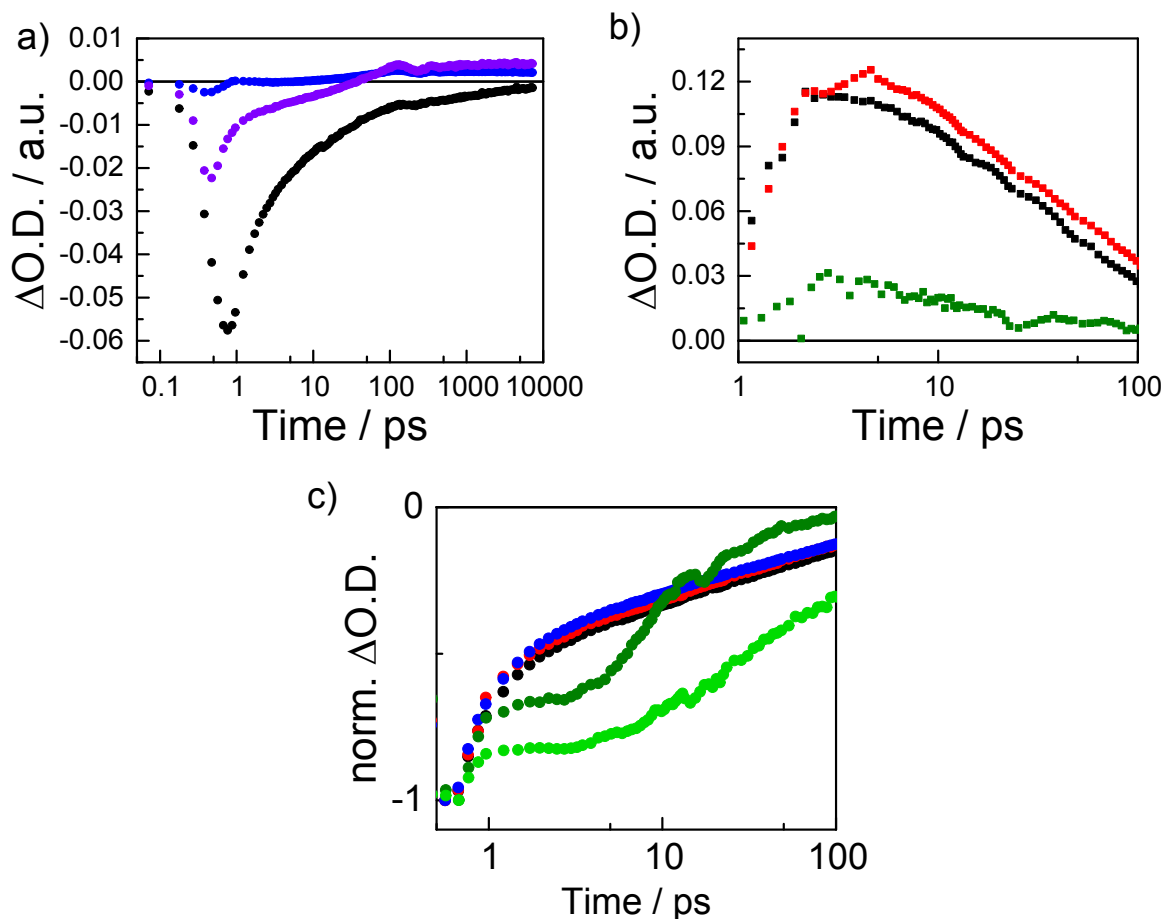


Figure S4. Transient absorption kinetic trace signals obtained upon femtosecond pump-probe experiments (775 nm) under inert atmosphere at room temperature. a) DPP measured at 705 nm (GSB; black), 557 nm (triplet excited state signal; blue), and 600 nm (singlet and maximum triplet excited state signal; purple); b) DPP's cation signal at 1437 nm for DPP:PC₆₁BM (black), DPP:FAPbI₃ (green), and DPP:FAPbI₃ (5 wt.%):PC₆₁BM (red), derived by subtracting the DPP's singlet excited state signal; c) Normalized kinetic traces of the ground state bleach signals of DPP:PC₆₁BM (black), DPP:FAPbI₃:PC₆₁BM with 5 wt.% (red) and 10 wt.% NCs (blue) at 704 nm, as well as DPP:FAPbI₃ at 681 nm (higher DPP content, dark green) and 756 nm (higher FAPbI₃ content, light green).

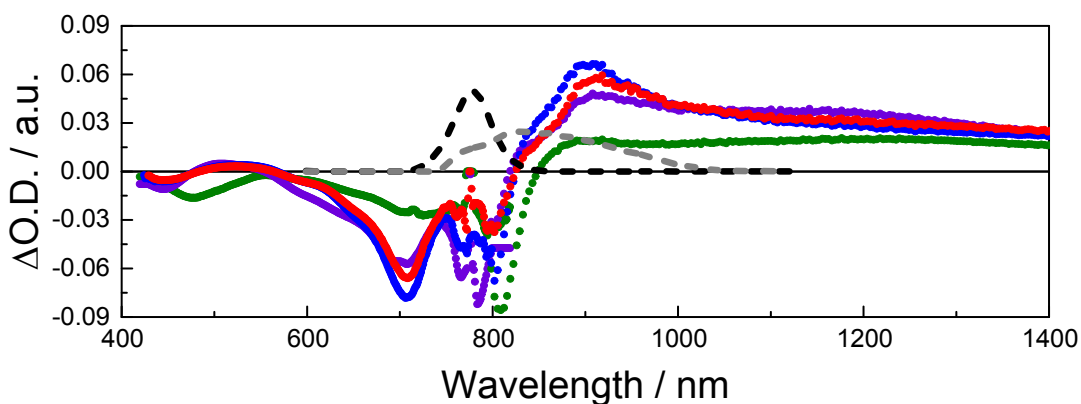


Figure S5. Circle symbols represent the differential absorption spectra obtained upon femtosecond pump-probe experiments (775 nm) under inert atmosphere at room temperature of DPP (purple), DPP:PC₆₁BM (blue), DPP:FAPbI₃ (3x enhanced, green), and DPP:FAPbI₃(5%):PC₆₁BM (red) after 600 fs. dashed lines are the PL spectra of DPP:FAPbI₃ (grey) and FAPbI₃ (black).

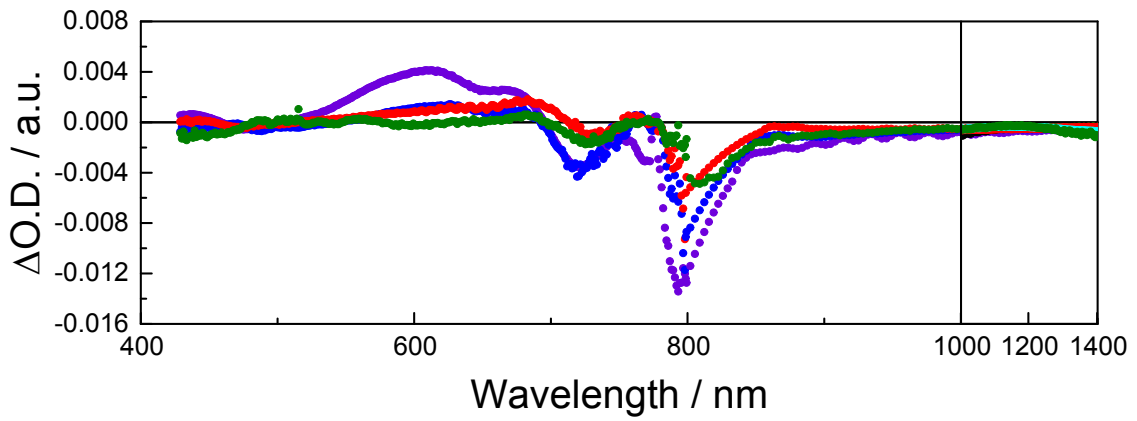
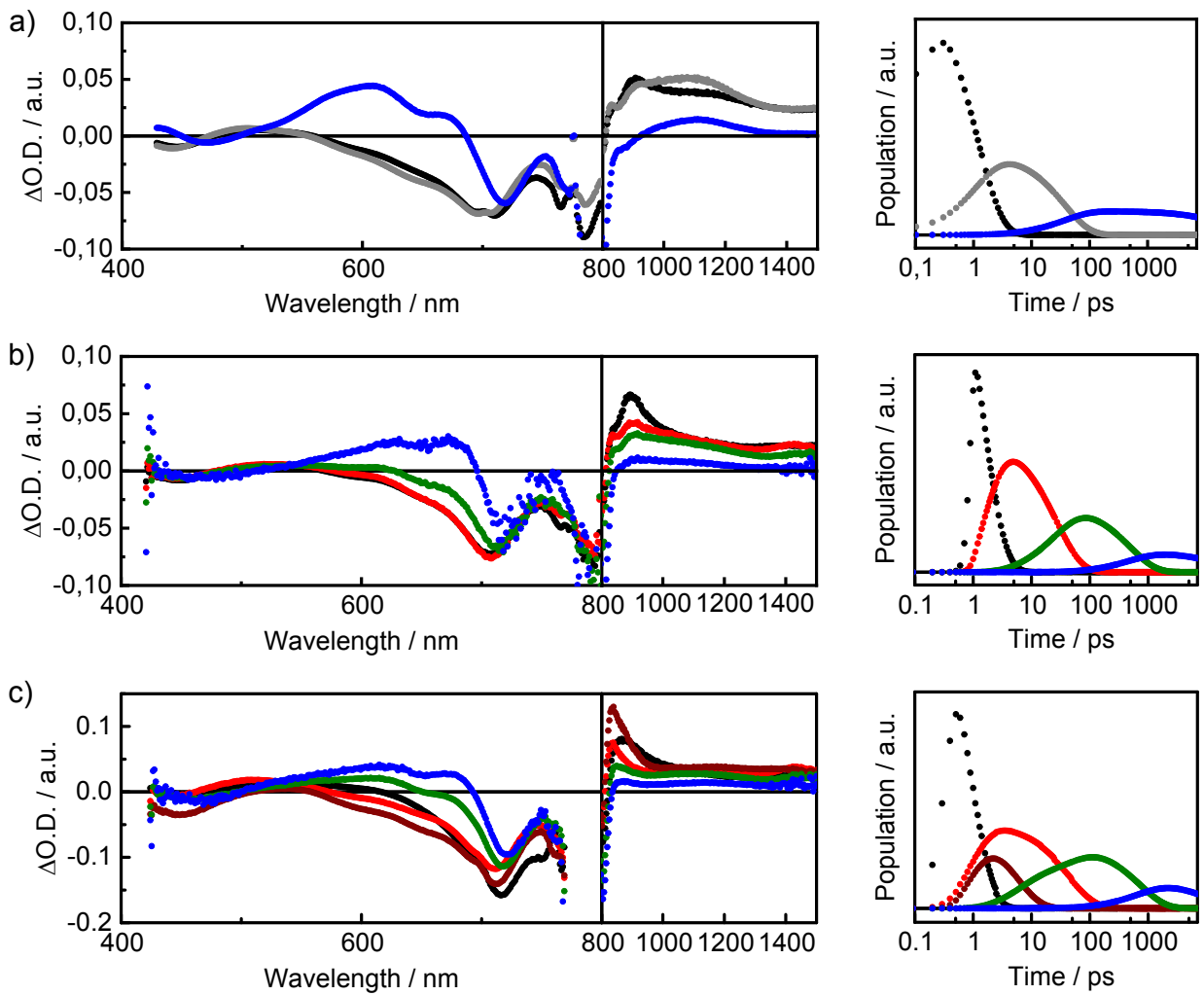


Figure S6. Differential absorption spectra of DPP (purple), DPP:PC₆₁BM (blue), DPP:FAPbI₃ (3x enhanced, green), and DPP:FAPbI₃(5%):PC₆₁BM (red) after 6 ns.



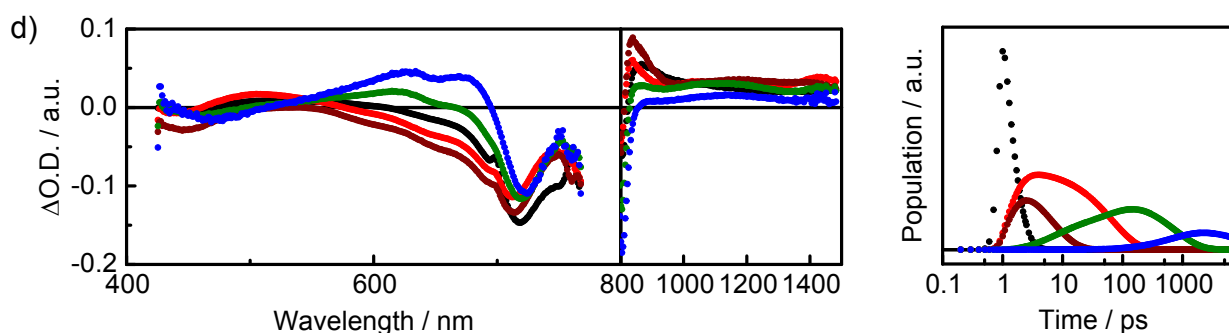


Figure S7. Species associated spectra (left) and state population (right) of a) DPP; b) DPP:PC₆₁BM; and c) ternary blends comprising 5 and d) 10 wt.% FAPbI₃ NCs showing DPP's singlet (black), intramolecular charge-transfer interaction of DPP (grey), the bound charge carriers located at the interface between DPP and either PC₆₁BM (red) or FAPbI₃ (dark red), the separated charge carriers in DPP and PC₆₁BM (green) as well as DPP's triplet (blue) like presented in the models.

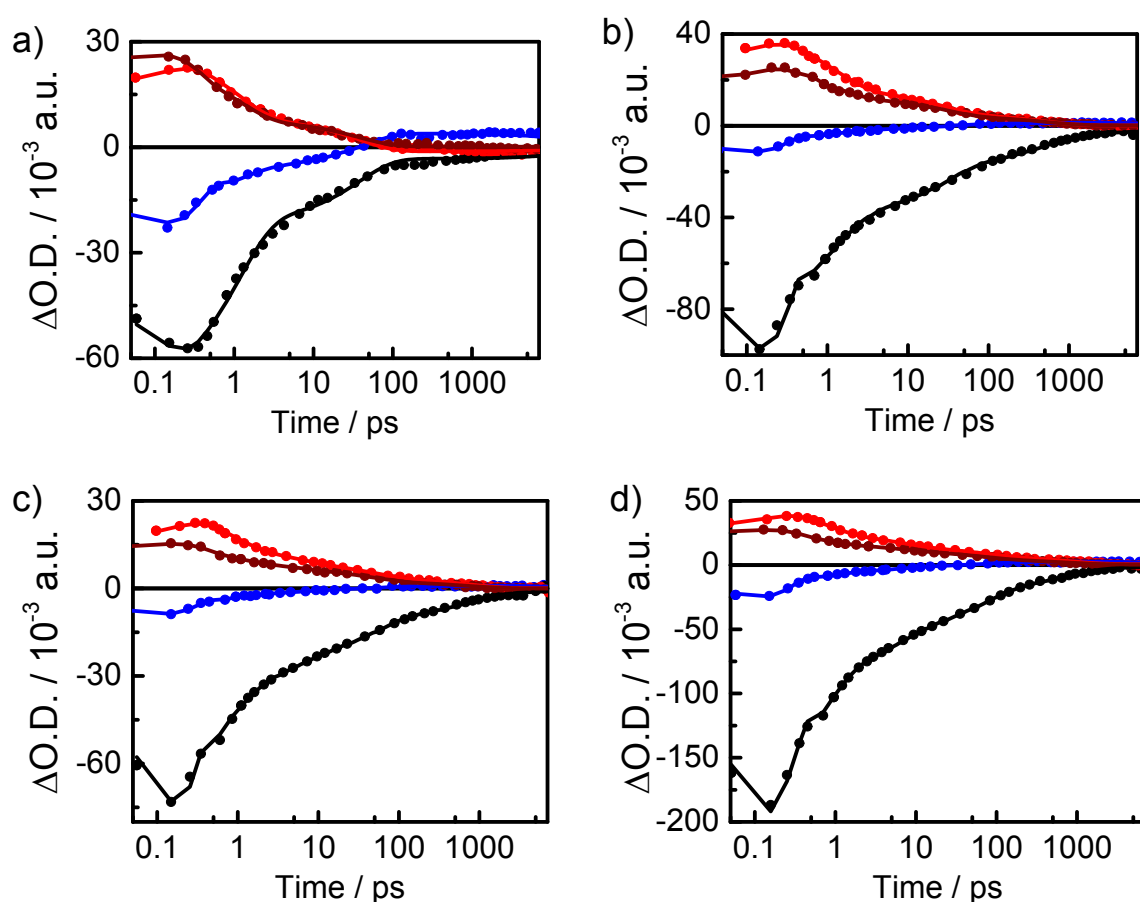


Figure S8. Differential absorption kinetics of a) DPP; b) DPP:PC₆₁BM; and c) ternary blends comprising 5 and d) 10 wt.% FAPbI₃ NCs showing the traces of the GSB (705 nm, black), the maximum of the triplet excited state peak (600 nm, blue), and the two main signals combining DPP's singlet excited state and cation (850 nm, light red; 1437 nm, dark red). The solid lines represent fitted curves using the model presented in Figure 6a, and a sequential one that includes radiative recombination for DPP.

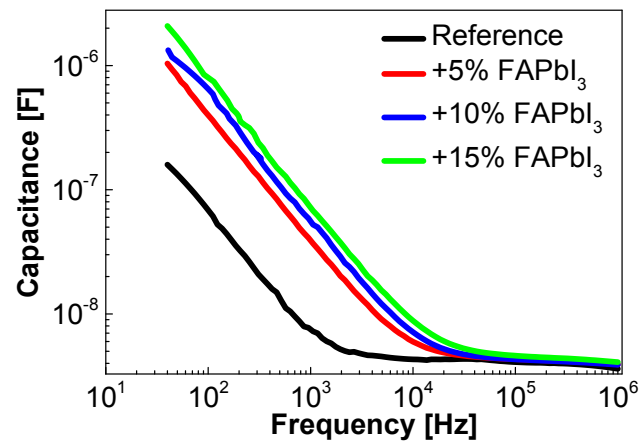


Figure S9. Capacitance as a function of frequency for the reference binary and ternary devices comprising various amount of FAPbI₃ perovskite NCs.